Nonlinear threshold behavior during the loss of Arctic sea ice

I. Eisenman[a,1,2] and J. S. Wettlaufer[b,c]

[a]Department of Earth and Planetary Sciences, Harvard University, Cambridge, MA 02138; [b]Department of Geology and Geophysics and Department of Physics, Yale University, New Haven, CT 96520; and [c]Nordic Institute for Theoretical Physics, Roslagstullsbacken 23, SE-106 91 Stockholm, Sweden

Edited by Carl Wunsch, Massachusetts Institute of Technology, Cambridge, MA, and approved November 14, 2008 (received for review July 25, 2008)

In light of the rapid recent retreat of Arctic sea ice, a number of studies have discussed the possibility of a critical threshold (or "tipping point") beyond which the ice–albedo feedback causes the ice cover to melt away in an irreversible process. The focus has typically been centered on the annual minimum (September) ice cover, which is often seen as particularly susceptible to destabilization by the ice–albedo feedback. Here, we examine the central physical processes associated with the transition from ice-covered to ice-free Arctic Ocean conditions. We show that although the ice–albedo feedback promotes the existence of multiple ice-cover states, the stabilizing thermodynamic effects of sea ice mitigate this when the Arctic Ocean is ice covered during a sufficiently large fraction of the year. These results suggest that critical threshold behavior is unlikely during the approach from current perennial sea-ice conditions to seasonally ice-free conditions. In a further warmed climate, however, we find that a critical threshold associated with the sudden loss of the remaining wintertime-only sea ice cover may be likely.

Arctic climate | bifurcation | climate change | tipping point

The retreat of Arctic sea ice during recent decades (1) is believed to be augmented by the difference in albedo (i.e., reflectivity) between sea ice and exposed ocean waters (2). Because bare or snow-covered sea ice is highly reflective to solar radiation, the increasing area of open water that is exposed as sea ice recedes leads to an increase in absorbed solar radiation, thereby contributing to further ice retreat. A number of recent studies have discussed the possibility that this positive ice–albedo feedback will cause the rapidly declining annual minimum (September) sea-ice cover to cross a critical threshold, after which the sea ice will melt back on an irreversible trajectory to a seasonally ice-free state (3–9).

Heuristically, one might expect in a simple annual mean picture of the Arctic Ocean that completely ice-covered and ice-free stable states could coexist under the same climate forcing. The ice-free state would remain warm because of the absorption of most incident solar radiation, whereas the ice-covered state would reflect most solar radiation and remain below the freezing temperature. In such a picture, these two stable states would be separated by an unstable intermediate state in which the Arctic Ocean is partially covered by ice and absorbs just enough solar radiation such that it remains at the freezing temperature: Adding a small amount of additional sea ice to this unstable state would lead to less solar absorption, cooling, and a further extended sea-ice cover. If the background climate warmed, the unstable state would require an increased ice extent to reflect sufficient solar radiation to remain at the freezing temperature. Beyond a critical threshold, the background climate would become so warm that the ice-covered state would reach the freezing temperature. At this point the stable ice-covered state and unstable intermediate state would merge and disappear in a saddle-node bifurcation, leaving only the warm ice-free state (10–12). This scenario suggests that if an ice-covered Arctic Ocean were warmed beyond the bifurcation point, there would be a rapid transition to the ice-free state. It would be an irreversible process in the sense that the Arctic Ocean would refreeze only after the climate had cooled to a second bifurcation point at which even an ice-free Arctic Ocean would become sufficiently cold to freeze, representing a significantly colder background climate than the original point at which the ice disappeared. Thus, the ice–albedo feedback could, in principle, cause a hysteresis loop in the Arctic climate response to warming.

Here, we investigate the central physical processes underlying the possibility of such a bifurcation threshold in future sea-ice retreat. We illustrate the discussion with a seasonally varying model of the Arctic sea ice–ocean–atmosphere climate system.

Arctic Sea Ice and Climate Model

The theory presented here describes the thermal evolution of sea ice, ocean mixed layer, and an energy balance atmosphere that is in steady-state with the underlying surface forcing, including also representations of dynamic sea-ice export and atmospheric meridional heat transport. The sea-ice thermodynamics in this model is an approximation of the full heat conduction equation of Maykut and Untersteiner (13), which provides the thermodynamic basis for most current sea ice models. Ice grows during the winter at the base, and when the surface reaches the freezing temperature in summer, ablation occurs at the surface as well as at the base. Our model produces an observationally consistent simulation of the modern Arctic sea ice seasonal cycle using a single 1-dimensional nonautonomous ordinary differential equation with observationally based seasonally varying parameters. Here we provide a brief summary of the model equations, which are fully derived from basic physical principles in the *SI Appendix*. The state variable E represents the energy per unit area stored in sea ice as latent heat when the ocean is ice covered or in the ocean mixed layer as sensible heat when the ocean is ice free,

$$E \equiv \begin{cases} -L_i h_i & E < 0 \text{ [sea ice]} \\ c_{ml} H_{ml} T_{ml} & E \geq 0 \text{ [ocean]} \end{cases}, \qquad [1]$$

where L_i is the latent heat of fusion for sea ice, h_i is the sea-ice thickness, c_{ml} is the mixed-layer specific heat capacity, and H_{ml} is the mixed-layer depth. The ocean mixed-layer temperature is written in terms of departure from the freezing point, $T_{ml} \equiv \tilde{T}_{ml} - \tilde{T}_{fr}$, where $\tilde{T}_{ml}$ is the ocean mixed-layer temperature and

Author contributions: I.E. and J.S.W. designed research, performed research, and wrote the paper.

The authors declare no conflict of interest.

This article is a PNAS Direct Submission.

[1]Present addresses: Division of Geological and Planetary Sciences, California Institute of Technology, Pasadena, CA 91125 and Department of Atmospheric Sciences, University of Washington, Seattle, WA 98195.

[2]To whom correspondence should be sent at the present address. E-mail: ian@gps.caltech.edu.

This article contains supporting information online at www.pnas.org/cgi/content/full/0806887106/DCSupplemental.

© 2008 by The National Academy of Sciences of the USA

Downloaded from https://www.pnas.org by WOODS HOLE OCEAN INST LIBRARY MARINE BIOLOGICAL LAB on November 13, 2023 from IP address 128.128.122.154.

$\tilde{T}_{fr}$ is taken to be 0 °C. The time evolution of E is proportional to the net energy flux,

$$\frac{dE}{dt} = [1 - \alpha(E)]F_S(t) - F_0(t) + \Delta F_0 - F_T(t)T(t, E) + F_B + v_0\mathcal{R}(-E). \quad [2]$$

Here, the Stefan–Boltzmann equation for outgoing longwave radiation has been linearized in the surface temperature departure from the freezing point, $T(t, E) \equiv \tilde{T}(t, E) - \tilde{T}_{fr}$, as $F_0(t) + F_T(t)T(t, E)$, where the parameters also account for the effects of a partially opaque atmosphere and atmospheric heat flux convergence that is a function the meridional temperature gradient. The seasonally varying values of $F_0(t)$ and $F_T(t)$ are derived by using an atmospheric model that incorporates observations of Arctic cloudiness (14), surface air temperature south of the Arctic (15), and atmospheric transport into the Arctic (16).

The term ΔF_0 represents a specified perturbation to the surface heat flux, which is zero by default but can be increased to prescribe a warming in the model. Incident surface shortwave radiation $F_S(t)$ and basal heat flux F_B are specified at central Arctic values (13). The final term in Eq. **2** accounts for an observationally based constant ice export of $v_0 = 10\%$ year^{-1} (17) when ice is present ($E < 0$), with the ramp function $\mathcal{R}(x)$ defined to equal x when $x \geq 0$ and to equal 0 when $x < 0$.

The surface temperature $T(t, E)$ can evolve among 3 different regimes. (*i*) When ice is present ($E < 0$) and the surface temperature is below the freezing point [$T(t, E) < 0$], it is calculated from a balance between the energy flux above the ice surface and upward heat flux in the ice, $-[1 - \alpha(E)]F_S(t) + F_0(t) - \Delta F_0 + F_T(t)T(t, E) = -k_i T(t, E)/h_i = k_i L_i T(t, E)/E$. (*ii*) When the surface temperature warms to the freezing point [$T(t, E) = 0$], it remains at this point while the ice undergoes surface ablation. (*iii*) When the ice ablates entirely, the ocean mixed layer is represented as a thermodynamic reservoir by using $T(t, E) = T_{ml} = E/(c_{ml}H_{ml})$. Using the ramp function as a convenient notation for combining cases (*i*) and (*ii*), the surface temperature can be expressed as

$$T(t, E) = \begin{cases} -\mathcal{R}\left[\dfrac{(1 - \alpha_i)F_S(t) - F_0(t) + \Delta F_0}{k_i L_i/E - F_T(t)}\right] & E < 0 \\ \dfrac{E}{c_{ml}H_{ml}} & E \geq 0 \end{cases}. \quad [3]$$

The ocean is represented as either ice covered or ice free at any given time. To model the gradual transition between these regimes in a partially ice-covered Arctic Ocean, the albedo varies between values for ice (α_i) and ocean mixed layer (α_{ml}) with a characteristic smoothness given by the thickness parameter h_α,

$$\alpha(E) = \frac{\alpha_{ml} + \alpha_i}{2} + \frac{\alpha_{ml} - \alpha_i}{2}\tanh\left(\frac{E}{L_i h_\alpha}\right). \quad [4]$$

We also consider a partially linearized version of the model in which Eq. **3** is replaced with

$$T(t, E) = \frac{E}{c_{ml}H_{ml}} \quad [5]$$

and there is no ice export ($v_0 = 0$). This causes the model equations to be linear with the exception of the ice–albedo feedback (Eq. **4**).

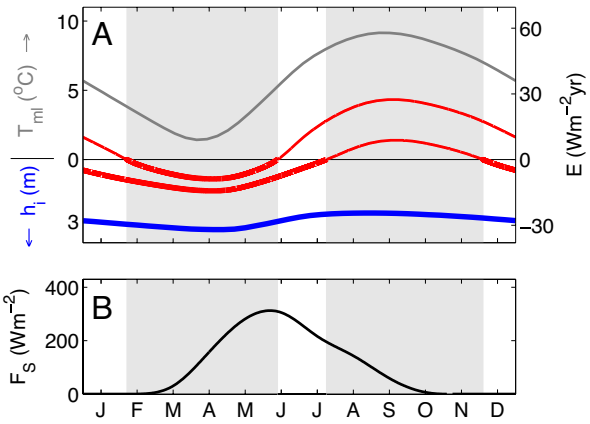

Fig. 1. Sea ice seasonal cycle in a warming climate and solar radiation. (*A*) Seasonal cycle of stable solutions of the full nonlinear model are illustrated by plotting the model state E (energy per unit area in ocean mixed layer sensible heat or sea ice latent heat) versus time of year. Four solutions are plotted, each with different levels of surface heating ΔF_0: a perennial ice state (blue curve, $\Delta F_0 = 0$), seasonally ice-free states with most of the year ice covered (lower red curve, $\Delta F_0 = 21$ Wm^{-2}) or most of the year ice free (upper red curve, $\Delta F_0 = 23$ Wm^{-2}), and a perennially ice-free state (gray curve, $\Delta F_0 = 19$ Wm^{-2}). As described in Eq. **1**, when $E > 0$, it represents the mixed-layer temperature of an ice-free ocean ($E = c_{ml}H_{ml}T_{ml}$). At $E = 0$, the ocean mixed layer reaches the freezing point ($T_{ml} = 0$ °C), and further cooling will cause ice to grow. When $E < 0$, it represents the sea-ice thickness ($E = -L_i h_i$); note that ice thickness increases downward. Model solutions are drawn with thicker lines when the ocean is ice covered and thinner lines when the ocean is ice free. Solutions are obtained by integrating Eqs. **2**–**4** with seasonally varying parameter values given in Table S1 in *SI Appendix* until the model has converged on a steady-state seasonal cycle. The light-gray shaded region to the right represents the first months to become ice free in a warming climate (demarcated by zero-crossings of the seasonally ice-free solution with $\Delta F_0 = 21$ Wm^{-2}), whereas the light-gray shaded region to the left represents the last months that are ice covered in a further warmed climate (demarcated by zero-crossings of the seasonally ice-free solution with $\Delta F_0 = 23$ Wm^{-2}). (*B*) Seasonal cycle of incident solar radiation specified in the model based on central Arctic surface observations (13), indicating that the first months to become ice free in a warming climate (light-gray region to right) and the last months to be ice covered in a further warmed climate (light-gray region to left) experience similar amounts of solar radiation. Note that the radiation curve is asymmetric because of seasonal differences in Arctic cloudiness, but the qualitative results presented here do not depend on this asymmetry.

Results

Seasonal Cycle. In a seasonally varying Arctic climate, warming might be expected to cause the sea ice to initially melt back to the point where the entire Arctic Ocean is ice free during part of the year, in contrast to the current perennial sea-ice cover in the central Arctic. Further warming would cause the ice-free period to increase until the Arctic Ocean becomes perennially ice free. We study this scenario theoretically by increasing the imposed surface heat flux ΔF_0 in Eqs. **2**–**4**. In Fig. 1*A*, steady-state seasonal cycle solutions are plotted in regimes with perennial ice cover (blue curve), seasonally ice-free conditions (red curves), and perennially ice-free conditions (gray curve).

The annual minimum sea-ice area and thickness is commonly referred to as "summer" sea ice, and the annual maximum is commonly referred to as "winter" sea ice. This nomenclature may carry with it the implication that the ice–albedo feedback, which depends on the magnitude of the incident solar radiation, would be most prominent during the retreat of the summer sea-ice cover. Indeed, it is often conjectured that a critical threshold for the loss of summer Arctic sea ice may be more likely than a threshold for the loss of winter ice (8). However, as is illustrated by Fig. 1*B*, this terminology can be misleading because the ice cover receives a similar amount of incident solar

Downloaded from https://www.pnas.org by WOODS HOLE OCEAN INST LIBRARY MARINE BIOLOGICAL LAB on November 13, 2023 from IP address 128.128.122.150.

Downloaded from https://www.pnas.org by WOODS HOLE OCEAN INST LIBRARY MARINE BIOLOGICAL LAB on November 13, 2023 from IP address 128.128.122.150.

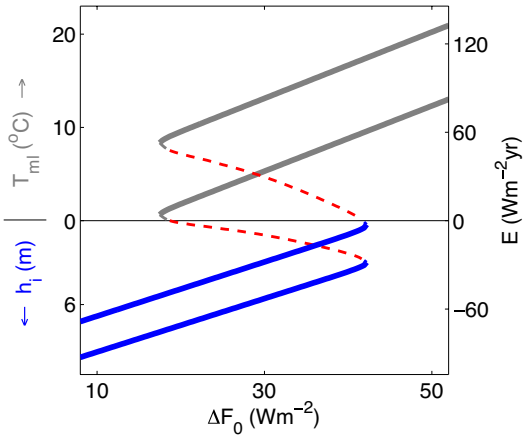

Fig. 2. Bifurcation diagram for the partially linearized model, where nonlinear sea-ice thermodynamic effects have been excluded but the ice–albedo feedback has been retained (Eqs. **2**, **4**, and **5**). For each value of the surface heating ΔF_0, the model is integrated until it converges on a steady-state seasonal cycle, and the annual maximum (upper curve) and annual minimum (lower curve) values of E are plotted. Solutions with perennial sea-ice cover are indicated in blue, seasonally ice-free solutions in red, and perennially ice-free solutions in gray. Dashed lines indicate unstable solutions, which have been determined by constructing an annual Poincaré map and finding the fixed points (i.e., numerically integrating the model for 1 year starting from an array of initial conditions and identifying the solutions with the same value of E at the end of the year as the initial condition). The curves have been smoothed with a boxcar filter to suppress a small level of noise associated with numerical integration. Note that the lines are slightly curved at the 2 bifurcation points because of the smooth albedo transition associated with $h_\alpha > 0$. The vertical axis is labeled as in Fig. 1*A*.

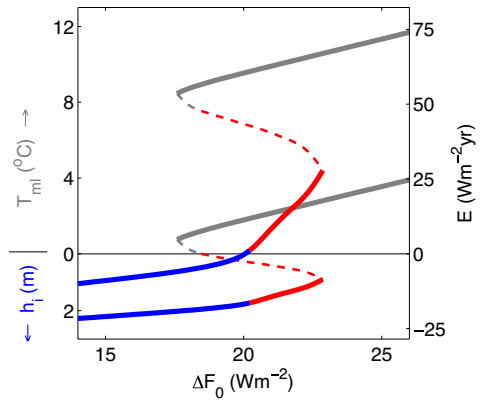

Fig. 3. Bifurcation diagram for the full nonlinear model (Eqs. **2**–**4**). Axes and colors are as described in the Fig. 2 legend. The inclusion of nonlinear sea-ice thermodynamic effects stabilizes the model when sea ice is present during a sufficiently large fraction of the year, allowing stable seasonally ice-free solutions (red solid curves). Under a moderate warming (ΔF_0 = 15 Wm^{-2}), modeled sea-ice thickness varies seasonally between 0.9 and 2.2 m. Further warming (ΔF_0 = 20 Wm^{-2}) causes the September ice cover to disappear, and the system undergoes a smooth transition to seasonally ice-free conditions. When the model is further warmed (ΔF_0 = 23 Wm^{-2}), a saddle-node bifurcation occurs, and the wintertime sea ice cover abruptly disappears in an irreversible process. Although the specific values of ΔF_0 at which the transitions occur are sensitive to parameter choices, the qualitative features of Fig. 3 are highly robust to changes in model parameter values (Fig. S4 in *SI Appendix*).

radiation during the period of annual maximum as at annual minimum. The light-gray shaded regions in Fig. 1 illustrate the key transition periods in the state of the Arctic Ocean during the transition from perennial ice cover to seasonally ice-free conditions (light gray region to right) and from seasonally ice-free conditions to perennially ice-free conditions (light gray region to left). Both of these periods experience approximately equivalent amounts of incident solar radiation (Fig. 1*B*), with somewhat more solar radiation occurring during the period associated with the loss of winter ice (light gray region to left). Hence the ice–albedo feedback should be expected to be similarly strong during a transition to perennially ice-free conditions in a very warm climate (i.e., loss of winter ice) as during a more imminent possible warming to seasonally ice-free conditions (i.e., loss of summer ice).

Bifurcation Thresholds. We begin the bifurcation analysis using the partially linearized version of the model (Eqs. **2**, **4**, and **5**) to focus on the effect of albedo in the absence of other nonlinearities. In this representation, the Arctic Ocean is viewed as a simple radiating thermal reservoir with a temperature-dependent albedo, and the model exhibits a linear relaxation to a stable solution in each albedo regime. As would be expected by analogy with the discussion above of an annual mean Arctic Ocean with a variable sea ice edge, Fig. 2 illustrates that when ΔF_0 becomes sufficiently large for the ocean to remain perennially ice free with $\alpha = \alpha_{ml}$, an unstable seasonally ice-free solution (red dashed curves) appears in a saddle-node bifurcation of cycles [for a discussion of the theory of bifurcations in periodic systems, see, e.g., Strogatz (18)].

The unstable solution separates stable solutions with perennial ice (blue curves) or perennially ice-free conditions (gray curves). The perennial ice regime collides with the unstable seasonally ice-free state and disappears in a second saddle-node bifurcation of cycles at the point where ΔF_0 becomes sufficiently large that the ice completely melts at the time of annual maximum E in the cold stable state. Because there is significant incident solar radiation during both the maximum and minimum periods of the seasonal cycle of E (Fig. 1), the ice–albedo feedback ensures that all seasonally ice-free solutions will be unstable (Fig. 2).

When nonlinear sea-ice thermodynamic effects are included (Eqs. **2**–**4**), basal ice formation is controlled by a diffusive vertical heat flux of $k_i\Delta T/h_i$, where ΔT is the difference between surface and basal temperatures and the base is assumed to be at the freezing point. This causes thin ice to grow significantly faster than thick ice (13). It would also cause thin ice to experience greater basal ablation during the summer melt season, but the surface temperature only warms until it reaches the freezing point ($\Delta T = 0$) and surface melt begins, making the rate of melt less sensitive to thickness. These 2 effects, both nonlinear in E, are expressed in Eq. **3** by the $-k_i/h = k_iL_i/E$ term in the denominator and the ramp function $\mathcal{R}(x)$, respectively. The result is an increase in the rate of growth for thin ice that is more stabilizing for thinner ice, as pointed out (19) and applied (20) in previous studies. This is in contrast to the state-independent linear mixed-layer stabilizing term, $-F_T(t)E/c_{ml}H_{ml}$, which applies when $E > 0$ (Eqs. **2** and **3**).

These nonlinearities allow for the existence of a stable seasonally ice-free solution (Fig. 3). When a sufficiently large value of ΔF_0 is chosen such that the cold solution becomes ice free during a small part of the year, a slight increase in temperature would lead to a longer open-water period and a thinner seasonal ice cover. Although the increased period of open water promotes warming through the ice–albedo feedback, the thinner ice grows significantly faster because of the sea-ice thermodynamic effects that are nonlinear in E. During the ice-covered portion of the year, the stability of the solution is controlled by this strong nonlinear stabilizing effect, but during the ice-free portion of the year, it is replaced by the weaker linear mixed-layer stabilizing term. This causes the stabilizing sea-ice thermodynamic effects to dominate the destabilizing ice–albedo feedback and allow a

stable seasonally ice-free solution only when there is ice cover during a sufficiently long portion of the year. Nonetheless, the ice–albedo feedback causes this regime to warm at an increased rate in response to increasing heat flux (compare slopes of red and blue curves in Fig. 3). As the ice-covered fraction of the year decreases in a warming climate, the stabilizing ice thermodynamic effects become less pronounced in the full annual cycle, and a bifurcation occurs when ice covers the Arctic Ocean during a sufficiently small fraction of the year to allow the ice–albedo feedback to dominate. Hence, when the Arctic warms beyond this point, the system supports only an ice-free solution (Fig. 3).

Discussion

Comparison with Results of Other Models. The theoretical treatment presented here is constructed to facilitate simple conceptual interpretation, and to this end many processes have been neglected. Factors including possible sea ice-cloud feedbacks (refs. 21–23 and D.S. Abbot, C.C. Walker, E. Tziperman, unpublished manuscript), the dependence of sea ice surface albedo on snow and melt pond coverage (24, 25), ocean heat flux convergence feedbacks (6, 26), changes in wind-driven ice dynamics (7), and changes in ice rheology (27) in a thinning ice cover (28) could potentially lead to other bifurcation thresholds or smooth out the threshold investigated here, akin to the smoothing of a first order phase transition because of statistical fluctuations (29). We are emboldened in our approach, however, because behavior consistent with the mechanism proposed here can be found in the published results of models with a broad range of complexities. (*i*) A "toy model" that is forced by a step-function seasonal cycle produced no stable seasonally ice-free solution in the published parameter regime (30), but by a slight adjustment of the tunable model parameters one can find a stable seasonally ice-free solution that coexists with a stable perennially ice-free solution (Fig. S5 in *SI Appendix*), consistent with the findings presented here. (*ii*) In a variant of the model used in this study that is significantly more complex (representing the simultaneous evolution of fractional Arctic sea-ice coverage, mean thickness, and surface temperature, as well as ocean mixed-layer temperature), increasing the level of greenhouse gas forcing leads to a gradual transition to seasonally ice-free solutions followed by a bifurcation threshold during the transition to perennially ice-free conditions (31), as in Fig. 3. (*iii*) Turning to the most complex current climate models, approximately half the coupled atmosphere–ocean global climate models used for the most recent IPCC report (32) predict seasonally ice-free Arctic Ocean conditions by the end of the 21st century, and none predict perennially ice-free conditions by the end of the 21st century. However, perennially ice-free Arctic Ocean conditions occur in 2 of the model simulations after CO_2 quadrupling. Neither of the models exhibits an abrupt transition when the annual minimum (September) ice cover disappears, but after further warming 1 of the models abruptly loses its March ice cover when it becomes perennially ice free (26). The physical mechanism presented here may help explain this abrupt simulated loss of March ice following the gradual simulated loss of September ice.

Conclusions. Our analysis suggests that a sea-ice bifurcation threshold (or "tipping point") caused by the ice–albedo feedback is not expected to occur in the transition from current perennial sea ice conditions to a seasonally ice-free Arctic Ocean, but that a bifurcation threshold associated with the sudden loss of the remaining seasonal ice cover may occur in response to further heating. These results may be interpreted by viewing the state of the Arctic Ocean as comprising a full seasonal cycle, which can include ice-covered periods as well as ice-free periods. The ice–albedo feedback promotes the existence of multiple states, allowing the possibility of abrupt transitions in the sea-ice cover as the Arctic is gradually forced to warm. Because a similar amount of solar radiation is incident at the surface during the first months to become ice free in a warming climate as during the final months to lose their ice in a further warmed climate, the ice–albedo feedback is similarly strong during both transitions. The asymmetry between these two transitions is associated with the fundamental nonlinearities of sea-ice thermodynamic effects, which make the Arctic climate more stable when sea ice is present than when the open ocean is exposed. Hence, when sea ice covers the Arctic Ocean during fewer months of the year, the state of the Arctic becomes less stable and more susceptible to destabilization by the ice–albedo feedback. In a warming climate, as discussed above, this causes irreversible threshold behavior during the potential distant loss of winter ice, but not during the more imminent possible loss of summer (September) ice.

The relevance of any basic theory to the actual future evolution of the complex climate system must be carefully qualified. Because the time scale associated with the sea-ice response to a change in forcing may be decadal, and the time scale associated with increasing greenhouse gas concentrations may be similar, the system may not be operating close to a steady-state. In the gradual approach to steady-state under a continual change in forcing, the difference between a region of the steady-state solution with increased sensitivity to the forcing and an actual discontinuous bifurcation threshold (as in Fig. 3) could be difficult to discern. If greenhouse gas concentrations were reduced after crossing a bifurcation threshold, however, the possible irreversibility of the trajectory would certainly be expected to be relevant.

ACKNOWLEDGMENTS. We thank the Geophysical Fluid Dynamics summer program at Woods Hole Oceanographic Institution (WHOI) [National Science Foundation (NSF) Grant OCE0325296], where the development of the physical representations used in this study benefited from discussions with many visitors and staff including Norbert Untersteiner, John Walsh, Jamie Morison, Dick Moritz, Danny Feltham, Göran Björk, Bert Rudels, Doug Martinson, Andrew Fowler, George Veronis, Grae Worster, Neil Balmforth, Ed Spiegel, Joe Keller, and Alan Thorndike. I.E. thanks Eli Tziperman and Cecilia Bitz for helpful conversations during the course of this work. The authors thank Richard Goody, Tapio Schneider, and Eli Tziperman for comments on the manuscript. J.S.W. acknowledges support from NSF Grant OPP0440841 and Yale University, and the Wenner–Gren Foundation, the Royal Institute of Technology, and NORDITA in Stockholm. I.E. acknowledges support from a National Aeronautics and Space Administration Earth and Space Science Fellowship, a WHOI Geophysical Fluid Dynamics Fellowship, NSF Paleoclimate Program Grant ATM-0502482, the McDonnell Foundation, a prize postdoctoral fellowship through the California Institute of Technology Division of Geological and Planetary Sciences, and a National Oceanic and Atmospheric Administration Climate and Global Change Postdoctoral Fellowship administered by the University Corporation for Atmospheric Research.

1. Stroeve JC, *et al.* (2005) Tracking the Arctic's shrinking ice cover: Another extreme September minimum in 2004. *Geophys Res Lett* 32:L04501.
2. Perovich DK, *et al.* (2007) Increasing solar heating of the Arctic Ocean and adjacent seas, 1979–2005: Attribution and role in the ice–albedo feedback. *Geophys Res Lett* 34:L19505.
3. Lindsay RW, Zhang J (2005) The thinning of Arctic sea ice, 1988–2003: Have we passed a tipping point? *J Clim* 18:4879–4894.
4. Overpeck J, *et al.* (2005) Arctic system on trajectory to new, seasonally ice-free state. *EOS* 86:309–313.
5. Serreze MC, Francis JA (2006) The Arctic amplification debate. *Clim Change* 76:241–264.
6. Holland MM, Bitz CM, Tremblay B (2006) Future abrupt reductions in the summer Arctic sea ice. *Geophys Res Lett* 33:L23503.
7. Maslanik J, *et al.* (2007) A younger, thinner arctic ice cover: Increased potential for rapid, extensive sea-ice loss. *Geophys Res Lett* 34:L24501.
8. Lenton TM, *et al.* (2008) Tipping elements in the Earth's climate system. *Proc Natl Acad Sci USA* 105:1786–1793.
9. Merryfield W, Holland M, Monahan A (2008) in *Arctic Sea Ice Decline: Observations, Projections, Mechanisms, and Implications*, eds DeWeaver E, Bitz CM, Tremblay B (Am Geophys Union), in press.
10. Budyko MI (1969) The effect of solar radiation variations on the climate of the earth. *Tellus* 21:611–619.

Downloaded from https://www.pnas.org by WOODS HOLE OCEAN INST LIBRARY MARINE BIOLOGICAL LAB on November 13, 2023 from IP address 128.128.122.150.

11. Sellers WD (1969) A global climate model based on the energy balance of the earth–atmosphere system. *J Appl Meteor* 8:392–400.
12. North GR (1990) Multiple solutions in energy-balance climate models. *Glob Planet Change* 82:225–235.
13. Maykut GA, Untersteiner N (1971) Some results from a time-dependent thermodynamic model of sea ice. *J Geophys Res* 76:1550–1575.
14. Maykut GA, Church PE (1973) Radiation climate of Barrow, Alaska, 1962–66. *J Appl Meteor* 12:620–628.
15. Kalnay E, *et al.* (1996) The NCEP/NCAR 40-year reanalysis project. *Bull Am Meteor Soc* 77:437–471.
16. Nakamura N, Oort AH (1988) Atmospheric heat budgets of the polar-regions. *J Geophys Res* 93:9510–9524.
17. Kwok R, Cunningham GF, Pang SS (2004) Fram Strait sea ice outflow. *J Geophys Res* 109:C01009.
18. Strogatz SH (1994) *Nonlinear Dynamics and Chaos* (Perseus Books, Jackson, TN).
19. Maykut G (1986) in *The Geophysics of Sea Ice*, ed Untersteiner N (Plenum, New York), pp 395–463.
20. Bitz CM, Roe GH (2004) A mechanism for the high rate of sea ice thinning in the arctic ocean. *J Clim* 17:3623–3632.
21. Kellogg WW (1975) in *Climate of the Arctic*, eds Weller G, Bowling SA (Geophys Inst, Univ Alaska, Fairbanks), pp 111–116.
22. Panel on Climate Change Feedbacks (2003) *Understanding Climate Change Feedbacks* (National Academies Press, Washington, DC).
23. Vavrus S (2004) The impact of cloud feedbacks on arctic climate under greenhouse forcing. *J Clim* 17:603–615.
24. Curry JA, Schramm JL, Ebert EE (1995) Sea-ice albedo climate feedback mechanism. *J Clim* 8:240–247.
25. Flato GM, Brown RD (1996) Variability and climate sensitivity of landfast Arctic sea ice. *J Geophys Res* 101:25767–25777.
26. Winton M (2006) Does the Arctic sea ice have a tipping point? *Geophys Res Lett* 33:L23504.
27. Zhang JL, Rothrock DA (2005) Effect of sea ice rheology in numerical investigations of climate. *J Geophys Res* 110:C08014.
28. Rothrock DA, Percival DB, Wensnahan M (2008) The decline in Arctic sea-ice thickness: Separating the spatial, annual, and interannual variability in a quarter century of submarine data. *J Geophys Res* 113:C05003.
29. Lifshitz EM, Pitaevskii LP (1980) *Statistical Physics* (Pergamon, Oxford).
30. Thorndike AS (1992) A toy model linking atmospheric thermal radiation and sea ice growth. *J Geophys Res* 97:9401–9410.
31. Eisenman I (2007) in *2006 Program of Studies: Ice (Geophysical Fluid Dynamics Program)* (Woods Hole Oceanogr Inst Tech Report 2007-02), pp 133–161 http://www.whoi.edu/page.do?pid=12938.
32. Solomon S, *et al.*, eds (2007) *Climate Change 2007: The Physical Science Basis. Contribution of Working Group I to the Fourth Assessment Report of the Intergovernmental Panel on Climate Change* (Cambridge Univ Press, Cambridge, UK), p 996.

Downloaded from https://www.pnas.org by WOODS HOLE OCEAN INST LIBRARY MARINE BIOLOGICAL LAB on November 13, 2023 from IP address 128.128.122.150.